Bioorganic Chemistry 83 (2019) 214–225

Contents lists available at ScienceDirect

Bioorganic Chemistry

journal homepage: www.elsevier.com/locate/bioorg

A novel bi-functional chalcone inhibits multi-drug resistant *Staphylococcus aureus* and potentiates the activity of fluoroquinolones

Vivek Kumar Gupta[a], Rashmi Gaur[b], Atin Sharma[a], Jawed Akther[a], Mahak Saini[a], Rajendra Singh Bhakuni[b], Ranjana Pathania[a,*]

[a] Molecular Bacteriology and Chemical Genetics Lab, Department of Biotechnology, Indian Institute of Technology Roorkee, District Haridwar, Uttarakhand 247667, India
[b] Medicinal Chemistry Division, CSIR-Central Institute of Medicinal and Aromatic Plants, Lucknow 226015, India

ARTICLE INFO

Keywords:
Antibacterial
Membrane disruption
Efflux pump inhibitor
Natural products
Proton motive force

ABSTRACT

Staphylococcus aureus is the leading cause of bacteraemia and the dwindling supply of effective antibacterials has exacerbated the problem of managing infections caused by this bacterium. Isoliquiritigenin (ISL) is a plant flavonoid that displays therapeutic potential against *S. aureus*. The present study identified a novel mannich base derivatives of ISL, IMRG4, active against Vancomycin intermediate *S. aureus* (VISA). IMRG4 damages the bacterial membranes causing membrane depolarization and permeabilization, as determined by loss of salt tolerance, flow cytometric analysis, propidium idodie and fluorescent microscopy. It reduces the intracellular invasion of HEK-293 cells by *S. aureus* and decreases the staphylococcal load in different organs of infected mice models. In addition to anti-staphylococcal activity, IMRG4 inhibits the multidrug efflux pump, NorA, which was determined by molecular docking and EtBr efflux assays. In combination, IMRG4 significantly reduces the MIC of norfloxacin for clinical strains of *S. aureus* including VISA. Development of resistance against IMRG4 alone and in combination with norfloxacin was low and IMRG4 prolongs the post-antibiotic effect of norfloxacin. These virtues combined with the low toxicity of IMRG4, assessed by MTT assay and haemolysis, makes it an ideal candidate to enter drug development pipeline against *S. aureus*.

1. Introduction

Methicillin-resistant *Staphylococcus aureus* (MRSA) is a major cause of community-acquired (CA-MRSA) and health care associated (HA-MRSA) infection outbreaks that range from severe to being potentially fatal [1]. MRSA and the recently emerged vancomycin-intermediate and resistant *S. aureus* (VISA and VRSA, respectively) have been listed as 'high-priority' deadly bacterial pathogens by the World Health Organization (WHO) [2]. Despite introduction of numerous drugs for the treatment of staphylococcal infections, the bacterium has been successful to resist the action of almost all classes of antibiotics including the latest classes, linezolid and daptomycin [3]. The mechanisms by which *S. aureus* evades the antibacterial action of antibiotics include, (i) enzymatic drug modification/inactivation, (ii) modification of drug binding site, (iii) acquisition of novel drug resistant target and (iv) overexpression of endogenous efflux pumps [4]. Efflux pumps are integral membrane based transport proteins which are involved in the extrusion of a broad range of structurally diverse antimicrobial agents. This results in reduced intracellular concentration to an ineffective level and subsequent cell survival [5]. Efflux pump transporters belong to five different families namely, Resistance Nodulation Division (RND) family; the Major Facilitator Superfamily (MFS); the ATP Binding Cassette (ABC) superfamily; the Small Multidrug Resistance (SMR) family; and the Multidrug And Toxic compound Extrusion (MATE) family. In Gram-positive bacteria, including *S. aureus*, MFS is the predominant family that utilizes an electrochemical gradient across the bacterial membrane for transporting drugs [6]. The well-studied native MFS efflux pump in *S. aureus*, NorA, is a proton motive force (PMF) dependent pump and is overexpressed in more than 50% of the resistant clinical isolates [7]. NorA confers resistance to a wide range of unrelated substrates such as hydrophilic fluoroquinolones (ciprofloxacin, norfloxacin), biocides (acriflavine, cetrimide, benzalkonium chloride) and dyes (ethidium bromide) [6]. Inhibition of NorA, therefore, is a possible strategy to combat the infections caused by MDR *S. aureus*. Natural plant products like reserpine [8], capsaicin [9], coumarins [10], chalcones [11], Boeravinone B [12] and some synthetic novel derivatives such as 1-(1H-indol-3-yl) ethanamine [13], Dithiazole thione derivatives [14] have been reported as potent NorA efflux pump inhibitors.

Isoliquiritigenin (ISL), a natural chalcone, was first isolated from the root of *Glycyrrhiza glabra* [15]. It has been reported for antimicrobial,

* Corresponding author at: Department of Biotechnology, Indian Institute of Technology Roorkee, Roorkee 247667, Uttarakhand, India.
E-mail address: rpathfbs@iitr.ac.in (R. Pathania).

https://doi.org/10.1016/j.bioorg.2018.10.024
Received 6 August 2018; Received in revised form 10 October 2018; Accepted 11 October 2018
Available online 17 October 2018
0045-2068/

anticancer, antioxidant, and anti-inflammatory activities [16]. Interestingly, the drug resistance reversal potential of ISL was recently reported [15] prompting us to synthesize novel derivatives of ISL using mannich base reaction and evaluate their antimicrobial and drug reversal potential against clinical strains of *S. aureus*. In the present study, we describe the role of a novel chalcone derivative as an antibacterial and an inhibitor of NorA efflux pump capable of rejuvenating the activity of fluoroquinolones.

2. Material and methods

2.1. Chemistry

Melting point was determined on a Toshniwal melting point apparatus. IR spectra were recorded on a Perkin Elmer 1719 FT-IR spectrophotometer. NMR spectra were obtained in $CDCl_3$, acetone-d_6, DMSO-d_6 and pyridine-d_5 on a Bruker Avance, 300 MHz instrument using TMS as internal standard. The chemical shift values are reported in ppm and coupling constants in Hz. ESI-MS spectra were recorded on a Perkin Elmer Turbo Mass/ Shimadzu LC-MS. TLC analyses were carried out on precoated silica gel 60 F_{254} plates (Merck) using solvent system, hexane: ethyl acetate (6:4). The compounds were visualized by either exposure of TLC plates to I_2 vapors or by spraying with vanillin-sulfuric acid reagent, followed by heating at 110 °C for 15 min. Si-gel, 60–120 mesh (spectrochem) was used in the column chromatography for the purification of metabolites and derivatives. The compounds were identified by their spectral IR, ID (^{1}H, ^{13}C, DEPT) and 2D (COSY, HSQC, HMBC) ESIMS) NMR and ESIMS analysis.

Isoliquiritigenin was isolated according to the reported procedure [15]. ISL derivatives IMRG1-IMRG6 were synthesized according to the procedure described below (Fig. 1).

N-Phenyl-N, 1a-dihydro-2H-O, N-isoliquiritigeninoxazine (IMRG1): It was obtained by refluxing ISL (0.256 g, 1 mmol), formaldehyde (0.2 mL, 2 mmol) and aniline (0.1 mL, 1 mmol) in methanol at 60 °C as a yellow solid (0.217 g, 85%), mp 70–72 °C. IR νmax (neat): 3448 (OH), 1654 (CO), 1602, 1562, 1510, 1366, 1223, 1032, 984 (aromatics), 1284, 1103 (ether) cm^{-1}; ^{1}H, COSY-NMR (400 MHz, Acetone-d_6): δ 4.63 (2H, s, H2-1a), 5.52 (2H, s, H2-2a), 6.38 (1H, d, J = 8.38 Hz, H-5″), 6.94 (3H, m, H-3′, H-5′, H-6a), 7.18 (2H, dd, J = 8.80, 2.0 Hz, H-4a, H-8a), 7.27 (2H, ddd, J = 8.76, 7.28, 2.16 Hz, H-5a, H-7a), 7.74 (2H, d, J = 8.88 Hz, H-2′, H-6′), 7.75 (1H, d, J = 14.96 Hz, H-2), 7.87 (1H, d, J = 15.32 Hz, H-3), 8.02 (1H, d, J = 9.04 Hz, H-6″); ^{13}C, DEPT-NMR (100 MHz, Acetone-d_6): δ 46.00 (C-1a), 80.68 (C-2a), 109.04 (C-5″), 109.66 (C-3″, q), 114.21 (C-1″, q), 116.81 (C-4a, C-8a), 117.99 (C-2), 118.95 (C-3′, C-5′), 122.18 (C-6a), 127.44 (C-1′, q), 130.04 (C-5a, C-7a), 130.52 (C-6″), 131.90 (C-2′, C-6′), 145.59 (C-3), 149.07 (C-3a, q), 161.18 (C-4′, q), 161.81 (C-2″, q), 163.29 (C-4″, q), 193.28 (C-1, q); ESI-MS (positive) (m/z): 374 [M + H]$^+$, molecular formula $C_{23}H_{19}O_4N$.

N-(p-Methylphenyl)-N, 1a-dihydro-2H-O, N-isoliquiritigeninoxazine (IMRG2): It was obtained by the reaction of ISL (0.256 g, 1 mmol), formaldehyde (0.2 mL, 2 mmol) and p-toluidine (0.107 g, 1 mmol) in methanol at 60 °C as a yellow solid (0.076 g, 30%), mp 75–77 °C. IR νmax (neat): 3367 (OH), 1654 (CO), 1602, 1545, 1511, 1460, 1366, 1219 (aromatics), 1166, 1101 (ether), 813 cm^{-1}; ^{1}H, COSY-NMR (300 MHz, Acetone-d_6): δ 2.27 (3H, s, CH_3), 4.52 (2H, s, H2-1a), 5.45 (1H, s, H2-2a), 6.31 (1H, d, J = 8.7 Hz, H-5″), 6.65 (2H, d, J = 8.4, H-3′, H-5′), 7.02 (5H, m, H-2, H-4a, H-5a, H-7a, H-8a), 7.54 (1H, d, J = 16.20 Hz, H-3), 7.80 (2H, d, J = 8.4 Hz, H-2′, H-6′), 8.01 (1H, d, J = 8.4 Hz, H-6″), 14.03 (1H, s, 4′-OH); 13C, DEPT-NMR (75 MHz, Acetone-d_6): δ 20.03 (CH_3), 46.38 (C-1a), 80.04 (C-2a), 108.56 (C-5″), 109.12 (C-3″, q), 114.08 (C-1″, q), 115.31 (C-3′, C-5′), 116.29 (C-2), 118.76, 119.05 (C-4a, C-8a), 126.01 (C-1′, q), 129.96 (C-6a, q), 130.03, (C-5a, C-7a, C-2′, C-6′), 131.39 (C-6″), 144.31 (C-3), 152.12 (C-3a, q), 160.05 (C-4′), 162.34 (C-2″), 166.02 (C-4″), 192.10 (C-1); ESI-MS (positive) (m/z): 388 [M + H]$^+$, molecular formula $C_{24}H_{21}O_4N$.

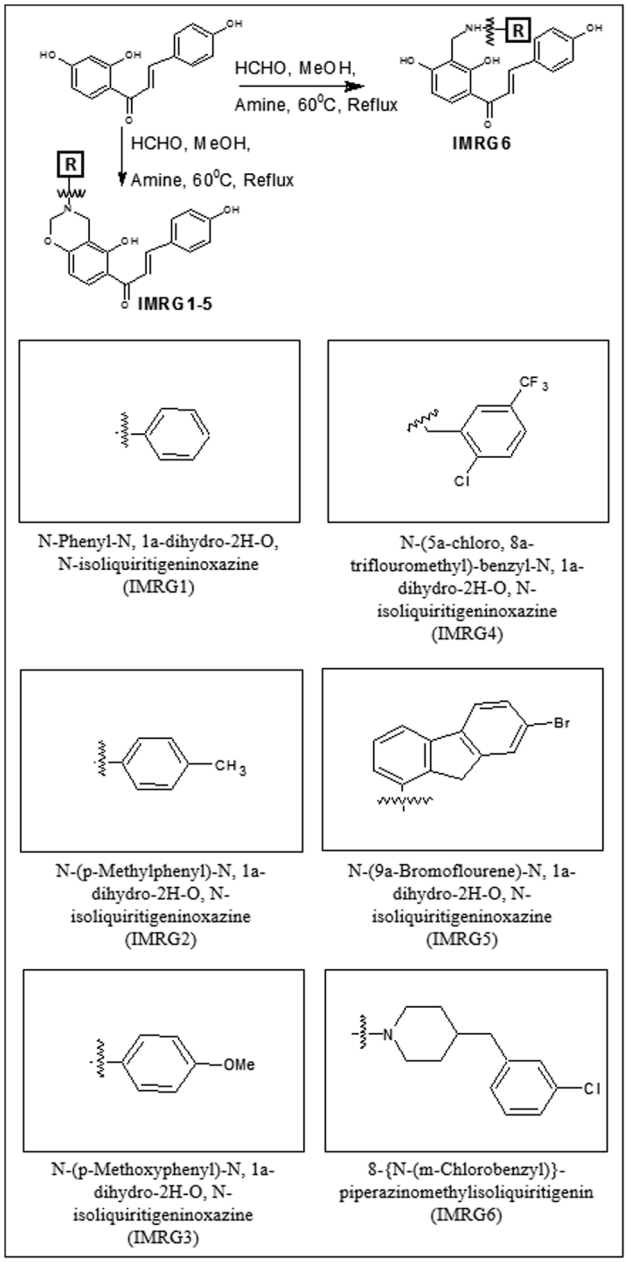

Fig. 1. Synthesis scheme and molecular structures of novel synthetic chalcone derivatives of ISL. The parent ISL moiety was modified to change the R group leading to different derivatives (IMRG1-6).

N-(p-Methoxyphenyl)-N, 1a-dihydro-2H-O, N-isoliquiritigeninoxazine (IMRG3): It was obtained by the reaction of ISL (0.256 g, 1 mmol), formaldehyde (0.2 mL, 2 mmol) and p-anisidine (0.123 g, 1 mmol) in methanol at 60 °C. It is a yellow solid (0.209 g, 82%), mp 135–137 °C. IR νmax (neat): 3398 (OH), 1655 (CO), 1590, 1545, 1460, 1043 (aromatics), 1113 (ether) cm^{-1}; ^{1}H, COSY-NMR (400 MHz, Acetone-d_6): δ 3.70 (3H, s, OCH_3), 4.54 (2H, s, H2-1a), 5.43 (2H, s, H2-2a), 6.34 (1H, d, J = 8.96 Hz, H-5″), 6.83 (2H, dd, J = 6.80, 2.30 Hz, H-3′, H-5′), 6.95 (2H, d, J = 8.64 Hz, H-4a, H-8a), 7.10 (2H, dd, J = 7.60, 2.30 Hz, H-5a, H-7a), 7.74 (2H, d, J = 8.84 Hz, H-2′, H-6′), 7.75 (1H, d, J = 14.88 Hz, H-2), 7.86 (1H, d, J = 15.36 Hz, H-3), 8.02 (1H, d, J = 9.00 Hz, H-6″); ^{13}C, DEPT-NMR (100 MHz, Acetone-d_6): δ 45.78 (C-1a), 54.79 (OCH_3), 80.94 (C-2a), 108.19 (C-5″), 108.71 (C-3″, q), 113.32 (C-1″, q), 114.34 (C-4a, C-8a), 115.96 (C-3′, C-5′), 117.22 (C-2), 120.24 (C-5a, C-7a), 126.59 (C-1′, q), 129.52 (C-6″), 131.03 (C-2′, C-6′), 141.95 (C-3a, q),

144.67 (C-3), 155.04 (C-6a, q), 160.31 (C-4′, q), 161.00 (C-2″, q), 162.45 (C-4″, q), 192.37 (C-1, q); ESI-MS (positive) (*m/z*): 404 $[M+H]^+$, molecular formula $C_{24}H_{21}O_5N$.

N-(5a-chloro, 8a-triflouromethyl)-benzyl-N, 1a-dihydro-2H-O, N-isoliquiritigeninoxazine (IMRG4): It was obtained by refluxing ISL (0.256 g, 1 mmol), formaldehyde (0.2 mL, 2 mmol) and 2-chloro-5-(triflouromethyl) benzylamine (0.1 mL, 1 mmol) in methanol at 60 °C as a yellow solid (0.204 g, 80%), mp 118–120 °C. IR νmax (neat): 3427, (OH), 1654 (CO), 1598, 1540, 1510, 1363, 1221, 1028, 983 (aromatics), 1171, 1083 (ether), 887, 830 cm^{-1}; ^1H, COSY-NMR (300 MHz, Acetone-d_6): δ 4.00, 4.15 (2H each, s, H2-1a, H2-3a), 5.08 (2H, s, H2-2a), 6.45 (1H, d, J = 8.7 Hz, H-5″), 6.95 (2H, d, J = 8.4, H-3′, H-5′), 6.77 (4H, m, H-2, H-3, H-2′, H-6′), 7.77 (3H, m, H-6a, H-7a, H-9a),), 8.08 (1H, d, J = 9.0 Hz, H-6″), 14.01 (1H, s, 4′-OH); ^{13}C, DEPT-NMR (75 MHz, Acetone-d_6): δ 44.66 (C-1a), 52.52 (C-3a), 83.83 (C-2a), 107.52 (C-3″), 108.08 (C-5″), 113.42 (C-1″, q), 115.87 (C-3′, C-5′), 117.22 (C-2), 125.47 (C-7a), 126.59 (C-1′, q), 126.88 (C-9a), 129.04 (C-8a, q), 129.60 (C-6a), 130.38 (C-6″), 131.00 (C-2′, C-6′), 137.71, 137.77 (C-4a, C-5a, q), 144.62 (C-3), 160.21 (C-4′, q), 160.70 (C-2″, q), 162.81 (C-4″, q), 192.31 (C-1, q); ESI-MS(positive): *m/z* 490 $[M+H]^+$, 512 $[M+Na]+$, 528 $[M+K]^+$, molecular formula $C_{25}H_{19}O_4NClF_3$.

N-(9a-Bromoflourene)-N, 1a-dihydro-2H-O, N-isoliquiritigeninoxazine (IMRG5): It was obtained by reacting isoliquiritigenin (0.256 g, 1 mmol), formaldehyde (0.2 mL, 2 mmol) and 2-amino-7-bromoflourene (0.324 g, 1 mmol) in methanol at 60 °C. It is a yellow solid (0.184 g, 72%), mp 118–120 °C. IR νmax (neat): 3401 (OH), 1655 (CO), 1601, 1562, 1510, 1367, 1227, 1034 (aromatics), 1169, 1099 (ether), 887, 830 cm^{-1}; ^1H, COSY-NMR (400 MHz, Acetone-d_6): δ 3.69 (2H, s, H2-6a), 4.83 (2H, s, H2-1a), 5.58 (2H, s, H2-2a), 6.59 (1H, d, J = 8.92 Hz, H-5″), 7.38 (1H, m, H-15a), 7.55 (3H, m, H-3′, H-5′, H-4a), 7.76 (5H, m, H-2, H-8a, H-10a, H-11a, H-14a), 7.80 (2H, m, H-2′, H-6′), 8.03 (1H, d, J = 9.04 Hz, H-6″), 8.20 (1H, d, J = 15.28 Hz, H-3); ^{13}C, DEPT-NMR (100 MHz, Acetone-d_6): δ 36.17 (C-6a), 46.17 (C-1a), 79.9 (C-2a), 108.57 (C-5″, C-15a), 109.29 (C-3″, q), 113.49 (C-1″, q), 116.77 (C-3′, C-5′), 117.17 (C-9a, q), 117.90 (C-2), 120.75 (C-4a), 126.31 (C-1′, q), 128.25, 128.57 (C-10a, C-11a, C-14a), 129.88 (C-8a, C-6″), 131.46 (C-2′, C-6′), 134.37 (C-13a, q), 140.93 (C-12a, q), 144.82 (C-3), 145.24, 145.35 (C-3a, 5a, q), 148.14 (C-7a, q), 161.07 (C-4′, q), 161.96 (C-2″, q), 162.76 (C-4″, q), 192.61 (C-1, q); ESI-MS (positive) (*m/z*): 540 $[M+H]^+$, (Negative): 538 $[M-H]^-$, molecular formula $C_{30}H_{21}O_4BrN$.

8-{N-(m-Chlorobenzyl)}-piperazinomethylisoliquiritigenin (IMRG6): It was obtained by the reaction of isoliquiritigenin (0.256 g, 1 mmol), formaldehyde (0.2 mL, 2 mmol) and 1-(3-chlorobenzyl)-piperazine (0.1 mL, 1 mmol) in methanol at 60 °C as a yellow solid (0.102 g, 40%), mp 118–120 °C. IR νmax (neat): 3399, 1655 (CO), 1596, 1544, 1460, 1422 (aromatics), 1120 (ether) cm^{-1}; ^1H, COSY-NMR (300 MHz, Acetone-d_6): δ 2.49, 2.60 (4H each, brs, H2-2a, H2-3a, H2-4a, H2-5a), 3.59 (4H, brs, H2-1a, H2-6a), 6.43 (1H, d, J = 8.7 Hz, H-5″), 6.91 (3H, m, H-2, H-3′, H-5′), 7.25 (3H, m, H-10a, H-11a, H-12a), 7.35 (1H, s, H-8a), 7.68 (2H, d, J = 8.4 Hz, H-2′, H-6′), 7.72 (1H, d, J = 15.3 Hz, H-3), 8.00 (1H, d, J = 8.7 Hz, H-6″); ^{13}C, DEPT-NMR (75 MHz, Acetone-d_6): δ 52.48, 52.76, 52.92, 53.50, 53.70, 53.84 (C-1a to C-6a), 108.12 (C-3″, q), 108.76 (C-5″), 114.01 (C-1″, q), 116.82 (C-3′, C-5′), 117.82 (C-2), 127.03 (C-1′, q), 127.50 (C-8a), 127.75, 128.29, 129.09 (C-12a/ C-11a/ C-10a), 130.25 (C-2′, C-6′), 131.28 (C-6″), 134.11, 141.29 (C-9a, C-7a, q), 144.56 (C-3), 158.07 (C-4′, q), 160.59 (C-2″, q), 166.18 (C-4″, q), 192.27 (C-1, q); ESI-MS (positive) (*m/z*): 479 $[M+H]^+$, 517 $[M+K]^+$, (Negative): 477 $[M-H]^-$, molecular formula $C_{27}H_{27}O_4N_2Cl$.

2.2. Bacterial strains

The bacterial strains including the clinical strains used in this study are mentioned in Supplementary Table S1. All the MRSA strains were verified for the presence of *mecA* gene by PCR amplification (Supplementary Fig. S1) [17].

2.3. In vitro antimicrobial susceptibility assay

Minimum inhibitory concentration (MIC) of ISL and its novel derivatives was determined by the broth microdilution method as per CLSI guidelines [18].

2.4. Time-kill studies

Time-kill kinetic study was performed to assess the bactericidal potential and synergistic interaction between most active derivative (IMRG4) and norfloxacin against *S. aureus* (SA-1199B, VISA-ST1745) as described earlier [19–21]. The criterion for a bactericidal effect was $\geq$3-$\log_{10}$ decrease in CFU count at a specified time while, a decline of less than 3-$\log_{10}$ CFU/ml was interpreted as bacteriostatic activity.

2.5. Salt tolerance assay

The salt tolerance of VISA-ST1745 was assessed in presence and absence of IMRG4 by observing the bacterial growth in agar medium supplemented with NaCl [22]. Detailed methodology can be found in Supplementary material SM1.

2.6. Cytoplasmic membrane depolarization assay

Fluorescent membrane-potential sensitive cyanine dye 3,3-dipropylthiacarbocyanine [$DiSC_3(5)$] was used to study membrane depolarization by IMRG4 [23]. Detailed methodology is mentioned in Supplementary material SM2.

2.7. Membrane permeabilization assay

The ability of IMRG4 to permeabilize the bacterial membrane was examined by PI uptake assay as per method described earlier and detailed in Supplementary material SM3 [24]. Microscopic determination of membrane integrity was made by using the LIVE/DEAD BacLight assay kit as per the manufacturer instructions.

2.8. Fluorescence microscopy

The mid log culture of VISA-ST1745 cells (OD600 = 0.6) were treated with 4× MIC of IMRG4, centrifuged and stained with 0.5-1 μg/ml N-(3-triethylammoniumpropyl)-4-(p-diethylaminophenyl-hexatrienyl) pyridinium dibromide (FM4–64, Molecular Probes). Samples were spotted on 2% agarose pads for imaging. Images were captured using a Zeiss Scope A1 fluorescence microscope, using the FM4–64 channel (λex = 540–580 nm; λem = 593–668 nm) as per method describe earlier [25].

2.9. Uptake of fluorescently labelled vancomycin

The mid log culture of VISA-ST1745 cells (OD_{600} = 0.6) was treated with 50 mg/L IMRG4 (4× MIC). After 4 h, treated cells as well as untreated control cells were harvested by centrifugation, washed thrice and resuspended in PBS. Cells were incubated with BODIPY-vancomycin (0.5× MIC) for 30 min at room temperature. After incubation, the cells were washed again with PBS to remove unbound BODIPY-vancomycin and resuspended in fresh PBS. The localization of BODIPY-vancomycin was analyzed by fluorescence microscopy using a green fluorescent protein filter (Nikon, Tokyo, Japan) as per method described by earlier [26].

2.10. Invasion assay

To ability of *S. aureus* cells (SA-1199B, VISA-ST1745 and SA-K1758) to invade HEK 293 (Human embryonic kidney cell lines) cells was assessed in presence and absence of IMRG4 as described earlier [9]. The details of the procedure are mentioned in Supplementary material SM4.

2.11. In vivo efficacy of IMRG4 in mice

The therapeutic efficacy of IMRG4 was evaluated through oral administration using *Swiss* albino mice model of *S. aureus* infection as described earlier [27]. Supplementary material SM5 contains the detailed methodology.

2.12. Checkerboard titration assay

The fractional inhibitory concentration (FICs) of ISL derivatives with different antibiotics was evaluated by modified broth checkerboard method [19,20]. The modified methodology has been detailed in Supplementary material SM6.

2.13. Computational assessment of NorA-IMRG4 interaction

The NorA sequence was used to prepare a 3D model and the using information of other known inhibitors of NorA, docking studies were performed to study interaction of IMRG4 with NorA. The detailed methodology has been given in Supplementary material SM7.

2.14. Ethidium bromide accumulation and efflux assay

Inhibition of NorA efflux pump by IMRG4 was studied by spectrofluorometric and flow cytometric determination of ethidium bromide accumulation and efflux assay previously described [28]. The methodology has been detailed in Supplementary material SM8.

2.15. In vitro ciprofloxacin/H^+ antiport assay

Everted membrane vesicles were prepared from NorA overexpressing cells (SA-1199B) as described previously with some modifications [29]. Ciprofloxacin/H^+ antiport activity was measured by the quinacrine fluorescence quenching method. The methodology has been detailed in Supplementary material SM9 and SM10.

2.16. Resistance development studies

The propensity of bacteria (VISA-ST1745) to develop resistance against IMRG4 alone and in combination with norfloxacin was evaluated as described earlier [30]. The methodology has been detailed in Supplementary material SM11.

2.17. Post antibiotic effect (PAE)

PAE was determined as described previously [29] and is detailed in Supplementary material SM 12.

2.18. Toxicity studies

The toxicity of IMRG4 was determined by haemolysis and MTT assay using HEK293 cell lines [29,31]. Detailed methodology has been given in Supplementary material SM13 and SM14 respectively.

3. Results

3.1. IMRG4, an ISL derivative, has potent anti-staphylococcal activity

Six novel ISL derivatives (IMRG1-6) were synthesized by Mannich base reaction method (Fig. 1). The antibacterial activity of ISL and its novel derivatives was assessed against different clinical strains of *S. aureus* (Table 1).

Table 1
Antibacterial activity of ISL and its novel derivatives (IMRG1-6) against clinical isolates of *S. aureus*.

S. aureus strains	MIC (mg/L)						
	ISL	IMRG1	IMRG2	IMRG3	IMRG4	IMRG5	IMRG6
SA-29213	50	25	100	> 100	50	100	> 100
SA-1199	50	50	100	> 100	25	50	100
SA-1199B	100	100	100	> 100	50	100	> 100
SA-K1758	50	50	100	> 100	25	50	100
MRSA-P4423	100	50	100	> 100	50	50	> 100
MRSA-P4627	100	50	100	> 100	25	50	> 100
MRSA-P4620	50	50	100	> 100	25	50	> 100
MRSA-B10760	100	50	> 100	> 100	50	100	> 100
MRSA-ST3151	50	50	> 100	> 100	25	50	> 100
VISA-ST2071	100	50	> 100	> 100	50	100	> 100
VISA-ST1745	100	100	100	> 100	50	100	> 100

Among the six derivatives, IMRG4 [N-(5a-chloro, 8a-triflouromethyl)-benzyl-N, 1a-dihydro-2H-O, N-isoliquiritigeninoxazine] exhibited significant antibacterial activity against all the tested strain of *S. aureus* with MIC values ranging from 25 to 50 mg/L. Since VISA-ST1754 displayed a wider antibiotic resistance profile among all the clinical isolates, it was used in further experiments (Supplementary Table S1). Time-kill assay, using the strain VISA-ST1745, showed that at MIC concentration, IMRG4 causes a 2-log reduction in the bacterial viability (in terms of bacterial CFU/ml) for upto 24 h. At higher concentrations of 2× and 4× MIC, as high as 4-log reduction in CFU/ml was observed after 24 h of incubation (Fig. 2a).

3.2. IMRG4 perturbs cytoplasmic membrane and causes membrane permeabilization

Preliminary assays were carried out to determine a probable mode of action of IMRG4. A significant reduction in the viability of *S. aureus* was found when the cells were grown in medium supplemented with 7.5% NaCl in the presence of IMRG4 (Fig. 2b). There was a mean 4-log reduction in bacterial salt tolerance (in terms of bacterial growth after 24 h in CFU/ml) when IMRG4 was added to the medium at MIC and 0.5× MIC concentrations. Since salt tolerance is a function of bacterial cell membrane, this observation hinted at damage to the membrane. Treatment of bacterial cells with IMRG4 resulted in an increased fluorescence of a cationic dye, DiSC3(5), similar to that in case of a known energy uncoupler, CCCP (Fig. 2c, d). In addition to membrane damage, this observation indicated dissipation of the bacterial membrane potential ($\Delta\Psi$) by IMRG4. Further fluorescent microscopic assays using propidium idodide (PI) showed an increased fluorescence and concomitant uptake by the bacterial cells. Untreated cells of *S. aureus* carried a little PI fluorescent signal, suggesting that they had intact and viable cell membranes (Fig. 2e). By contrast, a significant increase in PI fluorescent signal was observed in *S. aureus* cells treated with IMRG4, implicating that the membrane was permeabilized (Fig. 3a). The membrane disruption potential of IMRG4 was later validate by fluorescent microscopic assays using the membrane stain FM4-64. Deformed membranes with small bulge have been observed in IMRG4 treated cells as compared to untreated control cells (Fig. 3b). In addition, an increased in bodipy-vancomycin staining was observed at the septum in IMRG4 treated cells as compared to untreated control cells (Fig. 3c).

3.3. IMRG4 reduces the bacterial adhesion to eukaryotic cells and decreases bacterial load in infected organs in mice

The effect of IMRG4 on *S. aureus* was determined in terms of cellular

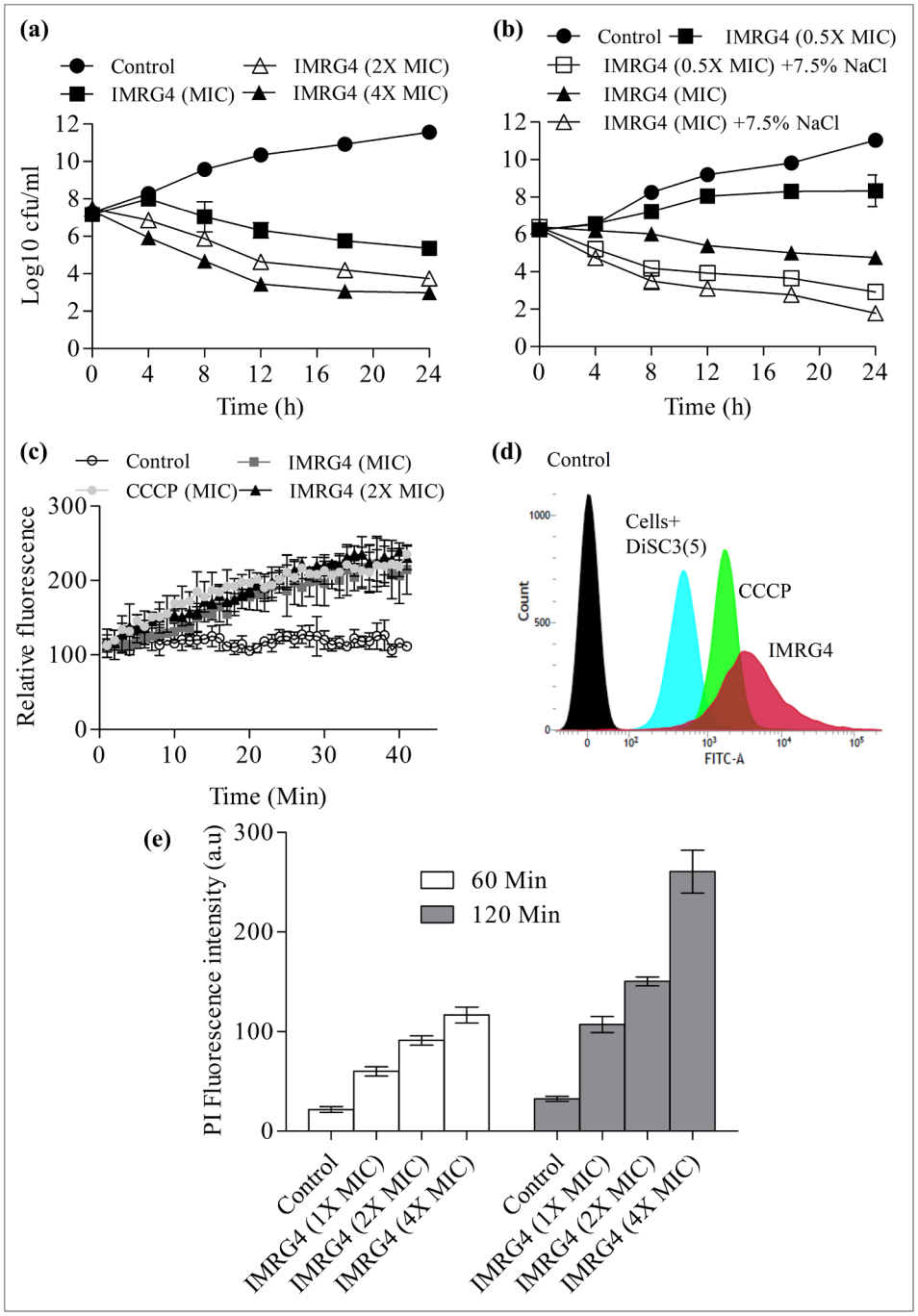

Fig. 2. Antibacterial and membrane disruption potential of IMRG4 (a) Time kill kinetic study of IMRG4 at different MICs against VISA-ST1745. At 1× MIC, IMRG4 reduces the growth of bacterial cells up to 2-folds (solid squares), while at 2× MIC and 4× MIC, it reduces the growth of bacterial cells up to 3-(open triangles) and 7-folds (solid triangles), respectively, in comparison to untreated cells (solid circle). Each point represents the mean of three different observations with the error bars representing SD. **(b) Loss of bacterial salt tolerance.** IMRG4 alone at 0.5× MIC and 1× MIC reduces the bacterial growth up to 1.3-fold (solid squares) and 2-folds (solid triangles), respectively, while at same concentration in presence of 7.5% NaCl (0.5× MIC + 7.5% NaCl, open squares and 1× MIC + 7.5% NaCl, open triangles) further 3-fold reduction in bacterial growth was observed, indicating membrane damaging potential of IMRG4. Each point represents the mean of three different observations with the error bars representing SD. **(c) Fluorimetric determination of membrane depolarization potential (Δψ) of IMRG4 at different MICs.** Dose dependent increase in fluorescence of [DiSC3(5)] was observed in IMRG4 [1× MIC (solid squares), 2× MIC (solid triangles)] treated cells in comparison to untreated cells (solid circle). CCCP (2.5 μM) was used as positive control (open circle). Each point represents the mean of three different observations with the error bars representing SD. **(d) Flow cytometric analysis of the effect of IMRG4 on membrane potential (Δψ).** 3,3-dipropylthiacarbocyanine [DiSC3(5)] fluorescence was analysed by flow cytometry using the FITC-A channel. Peaks have been labelled as per the constituents of the reaction mixtures. In IMRG4 treated cells, increase in florescence was observed similar to positive control CCCP. **(e) Propidium iodide uptake assay.** Fluorescence intensity of PI in bacterial cells treated with IMRG4 (at different concentrations) was determined by using spectrofluorometer at excitation and emission wavelengths of 493 nm and 636 nm, respectively. A significant increase in PI fluorescent signal was observed in cells treated with IMRG4 (dose dependent increase in PI fluorescence). Each bar represents the mean of three different observations with the error bars representing SD.

invasion and bacterial load in *S. aureus* infected mice model. The invasiveness of *S. aureus* cells was examined in the presence of IMRG4 at its subsub-MIC (0.25× MIC) concentration using HEK-293 cell lines. In the presence of IMRG4 there was more than 1-log reduction in invasiveness of *S. aureus* (Fig. 4a). *In vivo* anti-MRSA efficacy of IMRG4 was assessed using *Swiss* albino mice model. The staphylococcal load in various tissues upon treatment with IMRG4 at various doses (ranging from 50 to 6.25 mg/kg body weight) was determined. A dose-dependent significant reduction in microbial load was observed in different tissues including spleen, kidney, liver, and lung tissues (Fig. 4b). IMRG4, at a maximum dose of 50 mg/kg body weight, reduces the bacterial burden by a factor of 10 in spleen ($p < 0.001$), in kidney ($p < 0.001$), liver ($p < 0.001$) and lung ($p < 0.001$) as compared to the untreated control. Vancomycin was used as positive control which reduces the bacterial burden to a similar extent.

3.4. IMRG4 potentiates the activity of antibiotics when used in combination

The combinations of IMRG4 with different antibiotics and dyes like norfloxacin, ciprofloxacin tetracycline and EtBr showed profound synergy (Table 2, Supplementary Tables S4–S6).

There was a 4- to 20- fold reduction in MIC of norfloxacin when used in combination with IMRG4 against four clinical isolates, including *norA* overexpressor (SA-1199B) and knockout strain (SA-K1758) with fractional inhibitory concentration index (FICI) ranging from 0.30 to 0.49 (Supplementary Table S4). The IMRG4/ciprofloxacin combination showed synergistic interaction with 4- to 8-fold reduction against all tested clinical isolates (Supplementary Table S5). In combination with tetracycline also, IMRG4 exhibits synergistic interaction with 4- to 16-fold reduction against all tested clinical isolates and FICI ranging from 0.18 to 0.50 (Supplementary Table S6). Since IMRG4

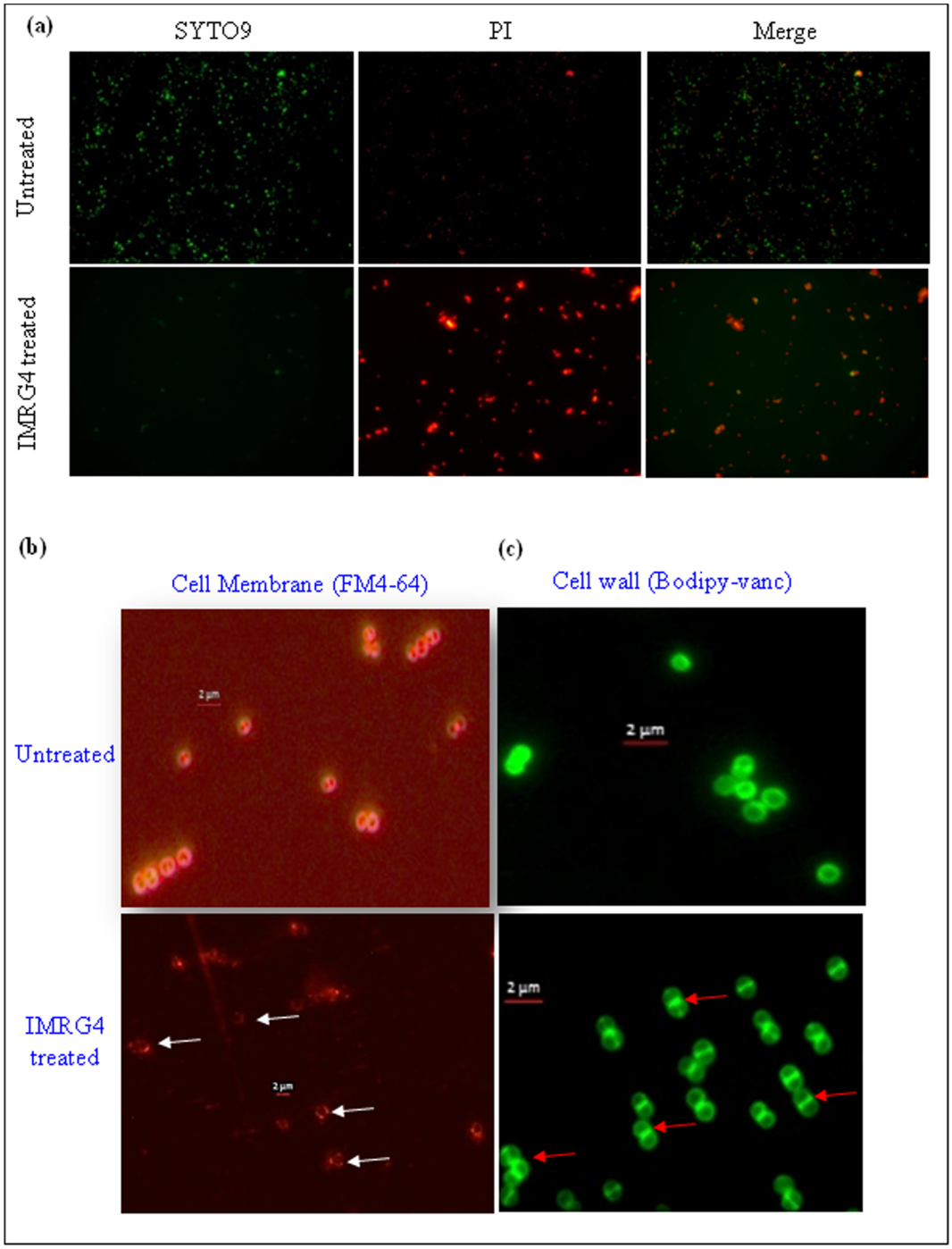

Fig. 3. Permeabilization of VISA-ST1745 membranes by IMRG4. (a) Fluorescence microscopy analysis for viability of bacterial cells using LIVE/DEAD BacLight bacterial viability assay kit. Bacterial cells were exposed to IMRG4 (4× MIC) for 2 h at 37 °C. Subsequently, the cells were washed with PBS and analysed by LIVE/DEAD BacLight bacterial viability assay kit. Microscopic images of representative IMRG4 treated and untreated bacterial cells were captured using Ziess Scope A1 microscope. Green fluorescence corresponds to the cells with intact membranes while red fluorescence corresponds to cells with permeabilized/damaged membranes cells. The data was normalized against the drug-free control. **(b) Fluorescence microscopy analysis for membrane disruption using the membrane stain FM4-64.** Bacterial cells were exposed to IMRG4 (4× MIC) for 8 h at 37 °C. Subsequently, the cells were washed with PBS and strain with FM4-64 (1 µg/mL). Deformed membranes with small bulge have been observed in IMRG4 treated cells as compared to untreated control cells. Scale bar corresponds to 2 µm. (**c**) **Fluorescence microscopic analysis for localization of BODIPY-vancomycin in VISA-ST1745.** Bacterial cells were treated with BODIPY-Van at 0.5× MIC concentration for 30 min, after incubation, the cells were washed with PBS and again resuspended in the same buffer. An increase in fluorescence was observed indicating the binding of BODIPY-Van only at bacterial cell surface. Bacterial cells were treated with IMRG4 (4× MIC) for 4 h and were further treated with BODIPY-Van (0.5× MIC) for another 30 min. After incubation, the cells were washed with PBS and again resuspended in the same buffer. An increase in bodipy-vancomycin staining was observed at the septum in IMRG4 treated cells as compared to untreated control cells (indicated by red arrows) which indicates that vancomycin might be diffuse towards septum (even at 0.5× MIC) in IMRG4 treated *S. aureus* cells. Scale bar corresponds to 2 µm.

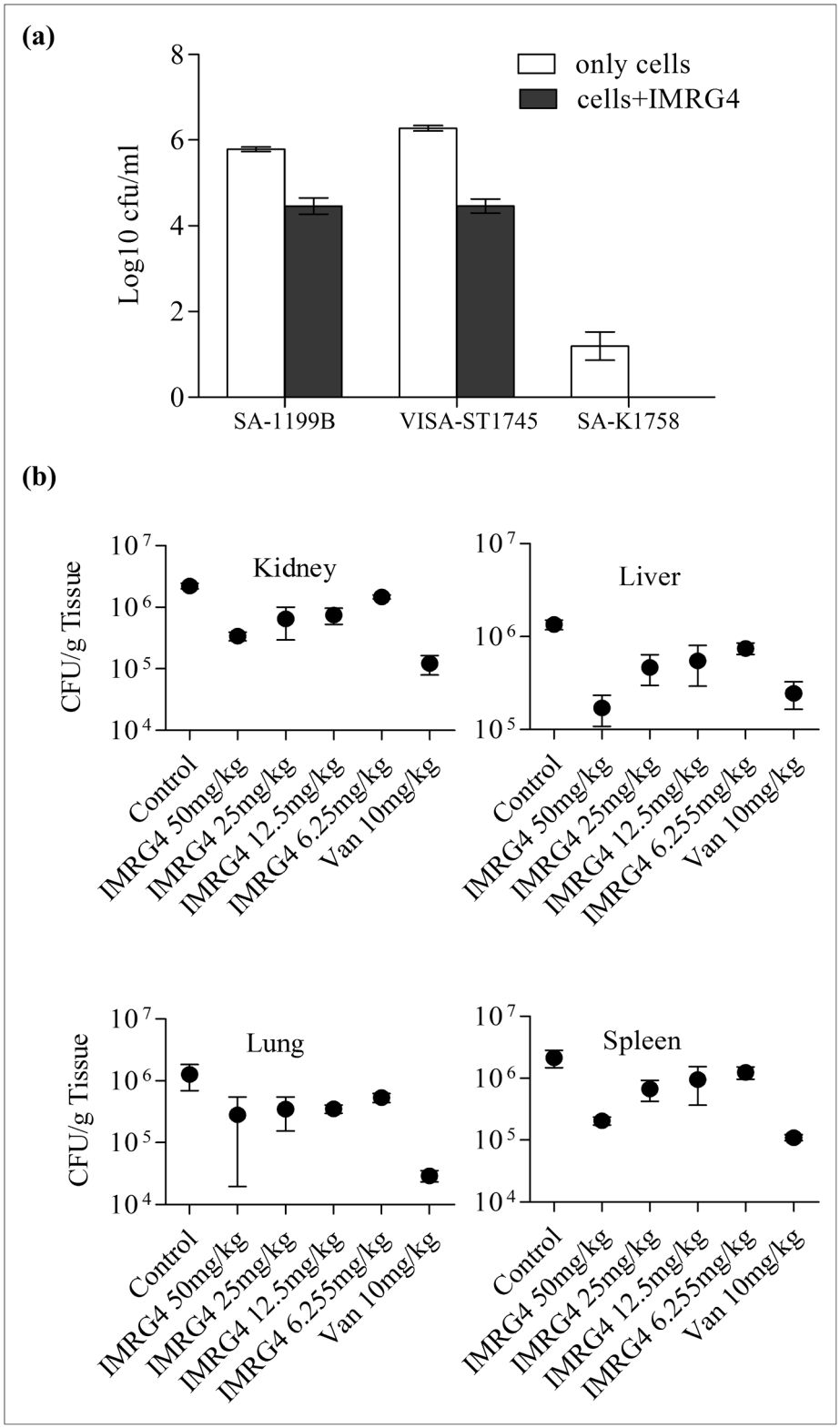

Fig. 4. Attenuation of *S. aureus* virulence (a) Influence of IMRG4 (0.25× MIC) (12.5 mg/L) on the invasive capacities of *S. aureus*, NorA-over-producing *S. aureus* SA-1199B, VISA ST-1745 and NorA knockout *S. aureus* SA-K1758. The invasiveness of SA-1199 and SA-1199B was significantly reduced in the presence of IMRG4. Each bar represents the mean of three different observations with the error bars representing SD. **(b) Bacterial load in different organs of VISA-ST1745 infected mice.** Mice were made neutropenic by administration of cyclophosphamide and were subsequently infected intravenously with 1×10^6 CFU/mL of VISA-ST1745. For the next 5 days, they were treated with the drugs (IMRG4 and vancomcin) following which they were sacrificed and the bacterial load in vital organs was determined. The control group only received vehicle. Data are expressed as mean ± SD ($p < 0.001$, ($p < 0.01$, ($p < 0.05$, Control v/s treatment group, Dunnett's Multiple Comparison Test).

exhibited up to 20-fold reduction in MIC of norfloxacin, the combination was used in further experiments. Bacterial kill kinetics revealed that IMRG4, in combination with norfloxacin at 0.25× MIC concentration, diminished the viability of SA-1199B (Fig. 5a) and VISA-ST1745 (Fig. 5b) by up to 3-log while at 0.5× MIC concentration, viability was reduced up to 7-log after 24 h of incubation. This is equivalent to the efficacy of norfloxacin alone at 4× MIC concentration (Fig. 5a and b).

3.5. IMRG4 inhibits NorA efflux pump

Synergy of IMRG4 with antibiotics that are substrates of an MDR efflux pump, NorA, hinted at interaction between IMRG4 and NorA. The NorA structure was modelled on 1PW4 and 3WDO PDB structures (Supplementary Fig. S2A). The quality of model was ensured by using Ramachandran plot and the model had 94% residues in the favoured region and no residue in disallowed region (Supplementary Fig. S2B).

Table 2
In-vitro interaction studies of novel ISL derivative (IMRG 4) with various antibiotics against clinical isolates of *S. aureus*. [Bold numbers indicate the synergistic interaction of IMRG4 with different antibiotics in terms of Fraction Inhibitory Concentration Index (FICI)]

S. aureus strain	Norfloxacin		Ciprofoloxacin		Tetracycline	
	Fold reduction	FICI	Fold reduction	FICI	Fold reduction	FICI
SA-1199	8	**0.380**	4	**0.500**	16	**0.203**
SA-1199B	16	**0.315**	4	**0.375**	16	**0.140**
SA-K1758	4	**0.499**	4	**0.500**	4	**0.375**
MRSA-P4423	20	**0.300**	8	**0.250**	8	**0.250**
MRSA-P4627	20	0.550	8	**0.375**	8	**0.375**
MRSA-P4620	10	0.550	4	**0.500**	4	**0.500**
MRSA-B10760	10	**0.350**	8	**0.250**	4	**0.375**
MRSA-ST3151	10	0.600	8	**0.375**	4	**0.500**
VISA-ST2071	20	**0.300**	8	**0.187**	8	**0.250**
VISA-ST1745	20	**0.300**	8	**0.187**	8	**0.250**

Docking studies performed using ciprofloxacin, norfloxacin, reserpine, IN-142, IN-203 and capsaicin on this model suggested that these substrates and inhibitors bind around the central hydrophobic cleft of trans-membrane domain. Our docking analysis suggests that IMRG4 also binds in the same hydrophobic cleft, interacting with Gln51, Val44, Ser337 (hydrogen bonding) Leu17, Ala48, Ala105, Met109 (hydrophobic interactions) with similar energies like the known inhibitors (Supplementary Fig. S3 and Table S7).

To assess the inhibition of NorA, fluorometric assays using ethidium bromide (EtBr) were carried out. In presence of IMRG4 (0.25× and 0.5× MIC), the accumulation of EtBr increased inside the bacterial cells over expressing NorA (Fig. 6a). A significant shift in the intensity of red fluorescence in the presence of IMRG4 as compared to untreated control was observed (Fig. 6b). The ability of IMRG4 (0.25× and 0.5× MIC) to inhibit the efflux of EtBr from bacterial cells was also evaluated. The NorA expressing cells were loaded with EtBr and the florescence was measured in presence and absence of IMRG4, once glucose was added to energize the pump. There was a rapid decrease in the fluorescence of untreated cells due to NorA-mediated EtBr efflux (Fig. 6c). In the presence of IMRG4, however, the loss of fluorescence was significantly reduced, reflecting inhibition of the efflux by IMRG4. No significant shift in the intensity of red fluorescence was observed inside the cells in the presence of IMRG4 (Fig. 6d). A similar effect was also recorded with a known efflux pump inhibitor, reserpine.

3.6. IMRG4 inhibits the drug/H + antiport movement across the bacterial membrane

NorA pump of *S. aureus* is driven by the H^+ gradient across bacterial membrane. To assess the effect of IMRG4 on drug/ H^+antiport movement across the membrane, a quinacrine-based fluorescence quenching assay was carried out using NorA enriched everted membrane vesicles of SA-1199B cells. The pumps were energized by the addition of lactate, resulting in an influx of H^+ ions and decrease in the fluorescence of quinacrine (Fig. 6e). Upon addition of ciprofloxacin, a substrate of NorA, the drug/ H^+antiport caused ciprofloxacin to move inside the vesicles in exchange for H^+ions, resulting in an increase in quinacrine fluorescence. This antiport was inhibited by addition of IMRG4, seen as a sharp increase in fluorescence of quinacrine. Thus, IMRG4 disrupts the proton gradient across the membrane causing an efflux of H^+ions from the everted membrane vesicles.

3.7. IMRG4 enhances the post antibiotic effect (PAE) and delays the appearance of resistance against norfloxacin

Since IMRG4 showed synergistic effect with fluoroquinolones and inhibited fluoroquinolones efflux through NorA, we assessed its utility as a therapeutic agent. Our results suggest that the clinical strains of *S. aureus* (VISA-ST1745) were not able to develop resistance against IMRG4 alone as well as in combination with norfloxacin even after 20 subsequent passages (Fig. 7a). A 2- to 8-fold increase in the MIC of IMRG4 alone was observed after 12 to 20 subsequent passages. However, in case of norfloxacin alone, upto 512-fold increase in MIC was observed during the same period (Fig. 7a). The post antibiotic effect (PAE) of IMRG4 and norfloxacin alone as well as in combination was determined at 0.5× MIC against the clinical strain VISA-ST1745 (Supplementary Table S8). IMRG4 and norfloxacin alone exhibited PAE of 24 min and 17 min respectively, which further increased up to 64 min in combination.

Cytotoxicity of IMRG4 was determined against human kidney embryonic cell lines (HEK-293). The percentage inhibition of cellular viability in presence of varying concentrations of IMRG4 was determined and the IC_{50} was calculated to be 281.63 mg/L (Fig. 7b). The IC_{50} is about 5 times higher than the MIC of IMRG4 against VISA-ST1745. Release of haemoglobin from human erythrocytes (RBCs) exposed to different concentrations of IMRG4 was also assessed to determine its toxicity. IMRG4 displayed no significant haemolytic activity upto 10× MIC concentration (Fig. 7c, Supplementary Fig. S4). In contrast, Triton X-100 completely lysed RBCs (100% haemolysis) significantly at a low concentration of 1% (v/v).

4. Discussion

Emergence and spread of multi-drug resistant clinical isolates of *S. aureus* represents a severe problem due to lack of effective therapeutic options [32]. Therefore, the development of novel antibacterial pharmacophores, which also delay the emergence of resistance, is required to combat such MDR infections. Plant phytochemicals have, in recent past, displayed their potential as antibacterial as well as drug resistance reversal agents. These phytochemicals frequently act through different mechanisms than conventional antibiotics [33,34]. Chalcones, including isoliquiritigenin (ISL), are one of those many phytochemicals with such reported activities [15,35]. Taking advantage of its properties, we synthesized novel derivatives of ISL using

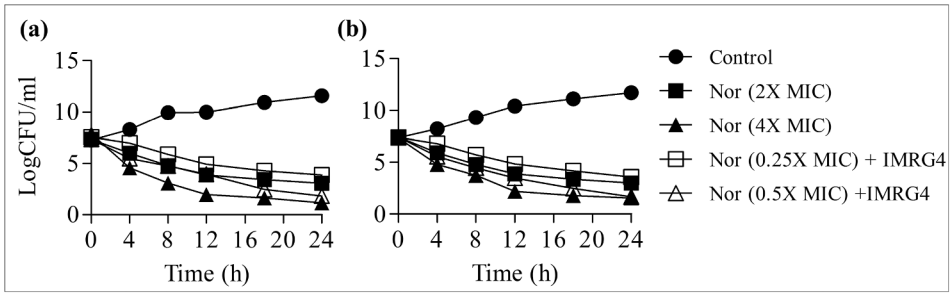

Fig. 5. Time kill kinetic study of norfloxacin in presence and absence of IMRG4. A sub-MIC concentration of norfloxacin with IMRG4 [0.25× MIC (Nor + IMRG4)] shows reduction in bacterial cells [SA-1199B (a), VISA-ST1745 (b)] by up to 3-folds (open squares) which was almost equivalent to norfloxacin (2× MIC, solid squares) treated cells, in comparison to untreated control cells (solid circles). At another sub-MIC concentration, norfloxacin in combination with IMRG4 [0.5× MIC (Nor + IMRG4)] shows bactericidal activity with reduction in growth of bacterial cells [SA-1199B (a), VISA-ST1745 (b)] by up to 7-folds (open triangles), similar to the activity of norfloxacin at 4× MIC (solid triangles). Each point represents the mean of three different observations with error bars representing SD.

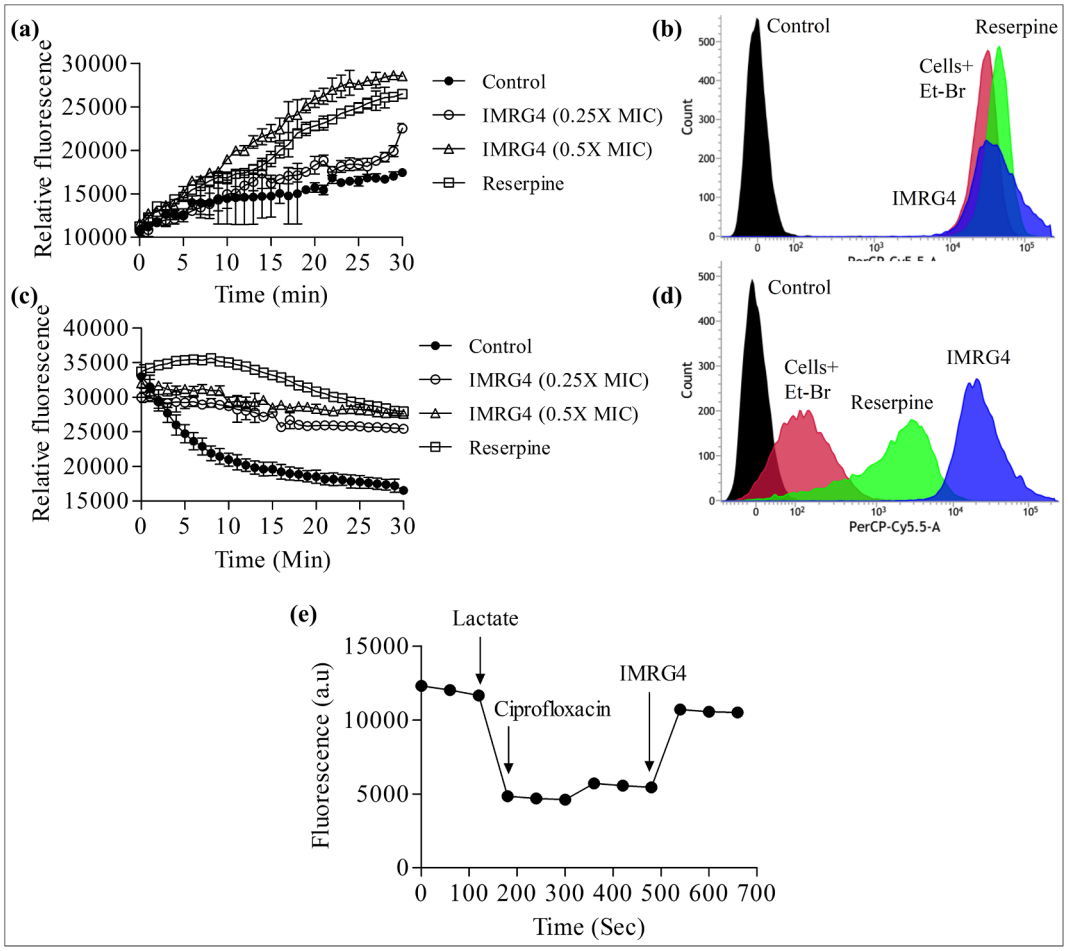

Fig. 6. Inhibition of NorA efflux pump by IMRG4 (a) The EtBr accumulation assay. Accumulation of EtBr inside SA-1199B cells was assessed. A dose dependent increase in fluorescence intensity was observed on addition of IMRG4 (0.25× MIC, open circles and 0.5× MIC, open trianlges) in comparison to untreated cells (solid circles). Similar observation was recorded with positive control reserpine (open squares). **(b) Flow cytometric assessment of EtBr accumulation.** Flow cytometric analysis also depicts the increase in EtBr fluorescence in the IMRG4 treated cells as a significant shift in the intensity of red fluorescence was observed inside the cells as compared to the untreated control. Similar observation was recorded with positive control reserpine **(c) The EtBr efflux inhibition assay.** Inhibition of EtBr efflux from SA-1199B cells loaded with EtBr was assessed in presence and absence of IMRG4. No significant decrease in fluorescence intensity was observed on addition of IMRG4 at different concentrations (0.25× MIC, open circles and 0.5× MIC, open triangles) in comparison to untreated cells (solid circles), where a significant decrease in fluorescence was observed. **(d) Flow cytometric assessment of EtBr efflux.** The flow cytometric analysis showed that IMRG4 significantly blocks the NorA-mediated EtBr efflux as no significant shift in the intensity of red fluorescence was observed inside the cells in the presence of IMRG4 as compared to control cells which efflux EtBr. **(e) Effect of IMRG4 on ciprofloxacin/H^+ antiport movement.** A quinacrine-based fluorescence quenching assay was carried out to monitor ciprofloxacin/H^+ antiport movement following the addition of IMRG4. Everted membrane vesicles were prepared from *norA* overproducing SA-1199B. Addition of Potassium lactate (5 mm) to the reaction mixture resulted in an influx of H^+ ions owing to respiration and a concomitant decrease in the fluorescence of quinacrine. After stabilisation ciprofloxacin was added (a substrate of NorA) to initiate the drug/H^+ antiport activity of NorA causing an increase in quinacrine fluorescence. The antiport was inhibited by addition of IMRG4, which disrupted the proton gradient across the membrane causing an efflux of H^+ ions as evident by a sharp increase in fluorescence of quinacrine. Each point represents the mean of three different observations with error bars representing SD.

mannich base reaction (Fig. 1). Out of the six derivatives, IMRG4 [N-(5a-chloro, 8a-triflouromethyl)-benzyl-N, 1a-dihydro-2H-O, N-iso-liquiritigeninoxazine] displayed a potent antibacterial activity against clinical isolates of *S. aureus* which included *mecA* positive MRSA, *norA* overexpressing strain (SA-1199B) and a *norA* deletion mutant (SA-K1758) of *S. aureus*. We determined that one of the strains, MRSA-ST1745, exhibits a vancomycin intermediate resistant phenotype, leading to its new designation as VISA-ST1745. This strain was used in further experimentation due to its broader antibiotic resistance profiling among all the tested clinical isolates of *S. aureus* (Supplementary Table S2).

From our experiments, it was revealed that IMRG4 acts on the bacterial membrane and its ability to depolarize the membrane was established by the membrane potential-sensitive fluorescent probe DiSC3(5) (Fig. 2). Further evidence of increase in membrane permeability and integrity were provided by microscopic visualization of PI uptake assay and membrane staining dye FM4-64 (Fig. 3a, 3b). Similar observations have been made using membrane active agents like, DNAC-1, SPI031 and DNAC-2 [25,36,37] against *S. aureus* suggesting that IMRG4 disrupts the bacterial membranes by combined action of membrane depolarization and membrane permeabilization. Several plant flavonoids like artonin I [38], 6,8-diprenyleriodictyol, isobavachalcone and 4-hydroxylonchocarpin [39] are also reported to diminish the viability of *S. aureus* via depolarizing the cytoplasmic membrane. Further, an increased in bodipy-vancomycin staining (even at sub-MIC) at the cell septum of virtually most of the IMRG4 treated cells (Fig. 3c), suggested that IMRG4 might affect the bacterial cell wall. Our observation led us to assume that IMRG4 may somehow also cause the thinning of the bacterial cell wall as BODIPY-vancomycin diffused easily towards septum in IMRG4 treated cells as compared to untreated control cells. However, further studies will be required to investigate the effect of IMRG4 on bacterial cell wall. Our findings are in

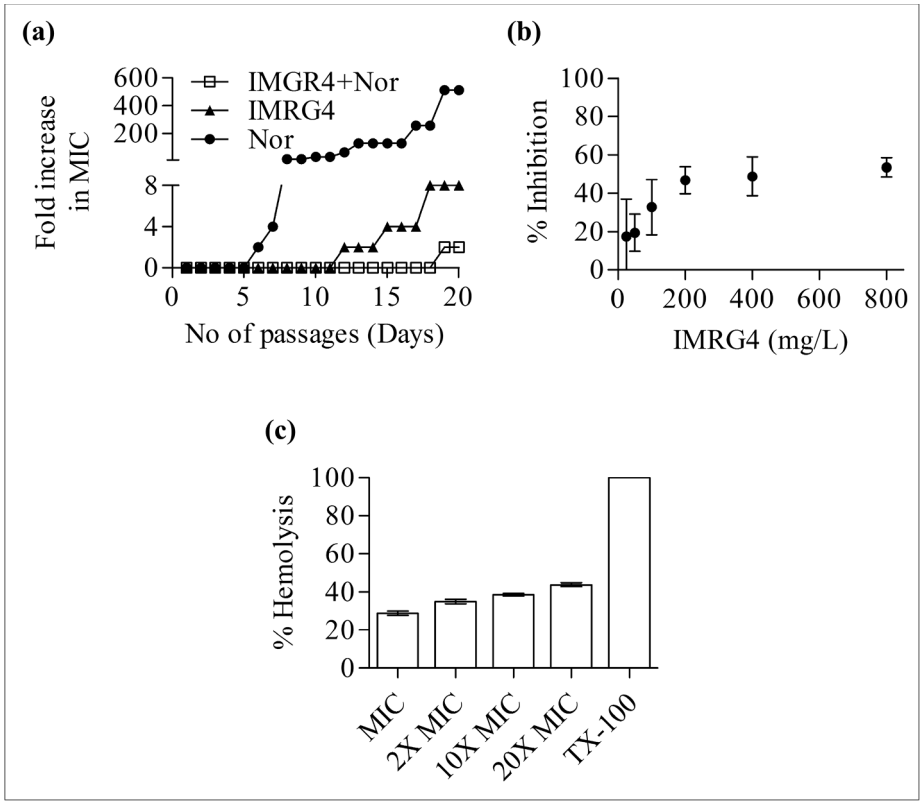

Fig. 7. Utility of IMRG4 as an adjuvant with norfloxacin (a) Generation of resistant mutants of *S. aureus* VISA-ST1745 against IMRG4 and norfloxacin alone as well as in combination. For each passage, the fold increase in MIC was determined by dividing MIC values of each passage by the initial MIC value (zero passage). *S. aureus* were not able to develop resistance against IMRG4 in combination with norfloxacin (open squares) after 20 passages whereas 2- to 8-fold increase in the MIC of IMRG4 (solid triangles) and 512-fold increase in MIC of norfloxacin alone (solid circles) was observed after 12 to 20 subsequent passages. **(b) Cytotoxicity of IMRG4.** MTT assay was carried out to determine the cytotoxicity of IMRG4 against human kidney embryonic cell lines (HEK-293). The percentage inhibition of cellular viability in presence of varying concentrations of IMRG4 was determined and the IC_{50} was calculated to be 281.63 mg/L. Each point represents the mean of six different observations with error bars representing SD. **(c) Haemolytic activity of the IMRG4 at different concentrations.** Release of haemoglobin from human erythrocytes (RBCs) exposed to different concentrations of IMRG4 was also assessed to determine its toxicity. Triton X-100 was used as a positive control. Each bar represents the mean of three different observations with the error bars representing SD.

accordance with previous reports [25,40,41].

Since *S. aureus* is a facultative intracellular pathogen and causes invasive disease, we assessed the effect of IMRG4 on bacterial invasion of animal cells [42]. The invasion of bacteria in presence of IMRG4 was significantly diminished *($p < 0.001$),* indicating the profound impact of IMRG4 on virulence of *S. aureus* (Fig. 4a). To further assess its antibacterial potential *in-vivo*, mice infected with VISA-ST1745 were treated with IMRG4 and a reduced bacterial load was reported in vital organs like kidney, liver, lung and spleen (Fig. 4b). Thus, IMRG4 was able to exert its antibacterial effect against VISA strain *in vitro* as well as *in vivo*.

Interestingly, IMRG4 displayed synergy with antibiotics like norfloxacin, ciprofloxacin and tetracycline (Table 2) and in a time kill assay, the combination of IMRG4 and norfloxacin at sub-MIC values was as effective as 2× and 4× MIC of norfloxacin alone (Fig. 5). Since norfloxacin and the other aforementioned antibiotics are substrates of a well-described MDR efflux pump, NorA [7], we hypothesized a role of IMRG4 in inhibition of NorA. Docking studies with an *in silico* model of NorA and IMRG4 indicated that IMRG4 could interact with the substrate binding pocket of NorA, similar to most of the reported efflux pump inhibitors (Supplementary Table S7). To validate our hypothesis, we carried out EtBr based assays which confirmed the ability of IMRG4 to potentiate the activity of norfloxacin via inhibiting the NorA efflux pump. Similar findings have been reported earlier [9] with a synthetic chalcone that inhibits NorA by disrupting the proton gradient. Bacteria maintain an electrochemical gradient across the membrane, proton motive force (PMF), which is a sum of two components, membrane potential (ΔΨ) and proton gradient (ΔpH) [43]. IMRG4 affected both ΔΨ and ΔpH which might form the basis of its antibacterial as well as efflux inhibition activity (Fig. 6). However, dissipation of both ΔΨ and ΔpH was expected to be toxic to the eukaryotic cells, much like in the case of CCCP. However, IMRG4 was significantly less toxic, with about 50% viability inhibition (of HEK-293 cells) at 800 mg/L (16× MIC) and less than 50% haemolysis at 1000 mg/L (20× MIC) concentrations (Fig. 6b and 6c). Synergistic interaction of two molecules that significantly dissipate both ΔΨ and ΔpH against MRSA has already been reported but the capability of both the activities in a single molecule is a unique property of IMRG4 (40). The invasiveness of NorA-overproducing *S. aureus* SA-1199B was reduced to a greater extent (up to 2-fold, Fig. 4a) as compared to the knockout strain (SA-K1758), an effect that can be explained by the fact that IMRG4 has a better activity against these strains due to inhibition of NorA efflux pump. Similar observations have been made by Hirakata et al [42] with diamine compounds which reduces the invasion of *P. aeruginosa* through the inhibition of MexAB-OprM pump. In addition to synergistic antibacterial activity with norfloxacin, the selection of resistant mutants as well as post-antibiotic effect of norfloxacin was delayed in presence of IMRG4. These findings, combined with the low toxicity of IMRG4, indicate that this molecule could be an ideal candidate to enter drug development pipeline.

Overall, our results collectively highlight the suitability of IMRG4 alone as well as in combination with fluoroquinolones like norfloxacin as a therapeutic agent for treatment of infections caused by MRSA/VISA. This study, for the first time, has shown that IMRG4 (novel mannich base derivative) diminishes the bacterial growth by a membranolytic mechanism including a combined action of membrane depolarization and membrane permeabilization. In addition to this IMRG4 can also potentiate the activity of fluoroquinolones by inhibiting the NorA efflux pump.

Acknowledgement

The authors are grateful to Prof. K. N. Prasad, Sanjay Gandhi Post Graduate Institute of Medical Sciences (SGPGIMS), Lucknow, India for providing the clinical isolates of *S. aureus* (MRSA/VISA). The authors are also thankful to Dr. Hemraj Nandanwar (CSIR-Institute of Microbial Technology, Chandigarh India for providing and to Prof. Glenn. W. Kaatz for agreeing to provide NorA overproducing strain (SA-1199B) and NorA knockout strain (SA-K1758). The authors also thankful to Prof. Partha Roy, Department of Biotechnology, Indian Institute of

Technology (IIT) Roorkee, Roorkee, Uttarakhand, India for human cell lines.

Ethical clearance

The animal experiment protocols (BT/IAEC/2017-20/06) were duly approved by Institutional Animal Ethics Committee on 31-03-2017.

Funding

This work was supported by DST SERB NPDF grant no. PDF/2016/000065 to V.K.G with R.P. as mentor. J.A. is financially supported by Indian Council of Medical Research, India.

Conflict of interest

None to declare.

Appendix A. Supplementary material

Supplementary data to this article can be found online at https://doi.org/10.1016/j.bioorg.2018.10.024.

References

[1] H.F. Chambers, F.R. DeLeo, Waves of resistance: *Staphylococcus aureus* in the Antibiotic Era, Nat. Rev. Microbiol. 7 (2009) 629–641, https://doi.org/10.1038/nrmicro2200.
[2] WHO publishes list of bacteria for which new antibiotics are urgently needed, World Health Organization, n.d. http://www.who.int/news-room/detail/27-02-2017-who-publishes-list-of-bacteria-for-which-new-antibiotics-are-urgently-needed (accessed July 26, 2018).
[3] T.J. Foster, Antibiotic resistance in *Staphylococcus aureus*. Current status and future prospects, FEMS Microbiol. Rev. 41 (2017) 430–449, https://doi.org/10.1093/femsre/fux007.
[4] J.M. Munita, C.A. Arias, Mechanisms of antibiotic resistance, Microbiol. Spectr. 4 (2016), https://doi.org/10.1128/microbiolspec.VMBF-0016-2015.
[5] M.A. Webber, L.J.V. Piddock, The importance of efflux pumps in bacterial antibiotic resistance, J. Antimicrob. Chemother. 51 (2003) 9–11, https://doi.org/10.1093/jac/dkg050.
[6] S.S. Costa, M. Viveiros, L. Amaral, I. Couto, Multidrug efflux pumps in *Staphylococcus aureus:* an update, Open Microbiol. J. 7 (2013) 59–71, https://doi.org/10.2174/1874285801307010059.
[7] C.E. DeMarco, L.A. Cushing, E. Frempong-Manso, S.M. Seo, T.A.A. Jaravaza, G.W. Kaatz, Efflux-related resistance to norfloxacin, dyes, and biocides in bloodstream isolates of *Staphylococcus aureus*, Antimicrob. Agents Chemother. 51 (2007) 3235–3239, https://doi.org/10.1128/AAC.00430-07.
[8] P.N. Markham, E. Westhaus, K. Klyachko, M.E. Johnson, A.A. Neyfakh, Multiple novel inhibitors of the NorA multidrug transporter of *Staphylococcus aureus*, Antimicrob. Agents Chemother. 43 (1999) 2404–2408.
[9] N.P. Kalia, P. Mahajan, R. Mehra, A. Nargotra, J.P. Sharma, S. Koul, I.A. Khan, Capsaicin, a novel inhibitor of the NorA efflux pump, reduces the intracellular invasion of *Staphylococcus aureus*, J. Antimicrob. Chemother. 67 (2012) 2401–2408, https://doi.org/10.1093/jac/dks232.
[10] S.K. Roy, N. Kumari, S. Pahwa, U.C. Agrahari, K.K. Bhutani, S.M. Jachak, H. Nandanwar, NorA efflux pump inhibitory activity of coumarins from *Mesua ferrea*, Fitoterapia 90 (2013) 140–150, https://doi.org/10.1016/j.fitote.2013.07.015.
[11] J.G. Holler, H.-C. Slotved, P. Mølgaard, C.E. Olsen, S.B. Christensen, Chalcone inhibitors of the NorA efflux pump in *Staphylococcus aureus* whole cells and enriched everted membrane vesicles, Bioorg. Med. Chem. 20 (2012) 4514–4521, https://doi.org/10.1016/j.bmc.2012.05.025.
[12] S. Singh, N.P. Kalia, P. Joshi, A. Kumar, P.R. Sharma, A. Kumar, S.B. Bharate, I.A. Khan, B. Boeravinone, A novel dual inhibitor of NorA bacterial efflux pump of *Staphylococcus aureus* and human P-glycoprotein, reduces the biofilm formation and intracellular invasion of bacteria, Front. Microbiol. 8 (2017) 1868, https://doi.org/10.3389/fmicb.2017.01868.
[13] A. Hequet, O.N. Burchak, M. Jeanty, X. Guinchard, E. Le Pihive, L. Maigre, P. Bouhours, D. Schneider, M. Maurin, J.-M. Paris, J.-N. Denis, C. Jolivalt, 1-(1H-indol-3-yl) ethanamine derivatives as potent *Staphylococcus aureus* NorA efflux pump inhibitors, ChemMedChem 9 (2014) 1534–1545, https://doi.org/10.1002/cmdc.201400042.
[14] R.C. Lowrence, T. Raman, H.V. Makala, V. Ulaganathan, S.G. Subramaniapillai, A.A. Kuppuswamy, A. Mani, S. Chittoor Neelakantan, S. Nagarajan, Dithiazole thione derivative as competitive NorA efflux pump inhibitor to curtail multi drug resistant clinical isolate of MRSA in a zebrafish infection model, Appl. Microbiol. Biotechnol. 100 (2016) 9265–9281, https://doi.org/10.1007/s00253-016-7759-2.
[15] R. Gaur, V.K. Gupta, P. Singh, A. Pal, M.P. Darokar, R.S. Bhakuni, Drug resistance reversal potential of isoliquiritigenin and liquiritigenin isolated from Glycyrrhiza glabra Against Methicillin-Resistant *Staphylococcus aureus* (MRSA), Phytotherapy Res. 30 (n.d.) 1708–1715. http://doi.org.10.1002/ptr.5677.
[16] F. Peng, Q. Du, C. Peng, N. Wang, H. Tang, X. Xie, J. Shen, J. Chen, A. Review, The pharmacology of isoliquiritigenin, Phytother. Res. 29 (2015) 969–977, https://doi.org/10.1002/ptr.5348.
[17] M.M. Pillai, R. Latha, G. Sarkar, Detection of Methicillin Resistance in *Staphylococcus aureus* by polymerase chain reaction and conventional methods: a comparative study, J. Lab Phys. 4 (2012) 83–88, https://doi.org/10.4103/0974-2727.105587.
[18] M07Ed11|Methods for Dilution Antimicrobial Susceptibility Tests for Bacteria That Grow Aerobically, 11th ed., Clinical & Laboratory Standards Institute, n.d. https://clsi.org/standards/products/microbiology/documents/m07/ (accessed July 26, 2018).
[19] P. Novy, J. Urban, O. Leuner, J. Vadlejch, L. Kokoska, *In vitro* synergistic effects of baicalin with oxytetracycline and tetracycline against *Staphylococcus aureus*, J. Antimicrob. Chemother. 66 (2011) 1298–1300, https://doi.org/10.1093/jac/dkr108.
[20] F.C. Odds, Synergy, antagonism, and what the chequerboard puts between them, J. Antimicrob. Chemother. 52 (2003) 1, https://doi.org/10.1093/jac/dkg301.
[21] V.K. Gupta, N. Tiwari, P. Gupta, S. Verma, A. Pal, S.K. Srivastava, M.P. Darokar, A clerodane diterpene from *Polyalthia longifolia* as a modifying agent of the resistance of methicillin resistant *Staphylococcus aureus*, Phytomedicine 23 (2016) 654–661, https://doi.org/10.1016/j.phymed.2016.03.001.
[22] V.K. Gupta, S. Verma, A. Pal, S.K. Srivastava, P.K. Srivastava, M.P. Darokar, In vivo efficacy and synergistic interaction of 16α-hydroxycleroda-3, 13 (14) Z-dien-15, 16-olide, a clerodane diterpene from *Polyalthia longifolia* against methicillin-resistant *Staphylococcus aureus*, Appl. Microbiol. Biotechnol. 97 (2013) 9121–9131, https://doi.org/10.1007/s00253-013-5154-9.
[23] H. Liu, M. Lei, X. Du, P. Cui, S. Zhang, Identification of a novel antimicrobial peptide from amphioxus *Branchiostoma japonicum* by *in silico* and functional analyses, Sci. Rep. 5 (2015) 18355, https://doi.org/10.1038/srep18355.
[24] P. Tyagi, M. Singh, H. Kumari, A. Kumari, K. Mukhopadhyay, Bactericidal activity of curcumin I is associated with damaging of bacterial membrane, PLoS One 10 (2015) e0121313, https://doi.org/10.1371/journal.pone.0121313.
[25] D.R. Nair, J.M. Monteiro, G. Memmi, J. Thanassi, M. Pucci, J. Schwartzman, M.G. Pinho, A.L. Cheung, Characterization of a novel small molecule that potentiates β-lactam activity against Gram-positive and Gram-negative pathogens, Antimicrob Agents Chemother. 59 (4) (2015) 1876–1885, https://doi.org/10.1128/AAC.04164-14.
[26] A. Singh, A. Ahmed, K.N. Prasad, S. Khanduja, S.K. Singh, J.K. Srivastava, N.S. Gajbhiye, Antibiofilm and membrane-damaging potential of cuprous oxide nanoparticles against *Staphylococcus aureus* with reduced susceptibility to vancomycin, Antimicrob. Agents Chemother. 59 (2015) 6882–6890, https://doi.org/10.1128/AAC.01440-15.
[27] V.K. Gupta, S. Verma, S. Gupta, A. Singh, A. Pal, S.K. Srivastava, P.K. Srivastava, S.C. Singh, M.P. Darokar, Membrane-damaging potential of natural L-(-)-usnic acid in *Staphylococcus aureus*, Eur. J. Clin. Microbiol. Infect. Dis. 31 (2012) 3375–3383, https://doi.org/10.1007/s10096-012-1706-7.
[28] A. Sharma, R. Sharma, T. Bhattacharyya, T. Bhando, R. Pathania, Fosfomycin resistance in *Acinetobacter baumannii* is mediated by efflux through a major facilitator superfamily (MFS) transporter-AbaF, J. Antimicrob. Chemother. 72 (2017) 68–74, https://doi.org/10.1093/jac/dkw382.
[29] T. Bhattacharyya, A. Sharma, J. Akhter, R. Pathania, The small molecule IITR08027 restores the antibacterial activity of fluoroquinolones against multidrug-resistant *Acinetobacter baumannii* by efflux inhibition, Int. J. Antimicrob. Agents 50 (2017) 219–226, https://doi.org/10.1016/j.ijantimicag.2017.03.005.
[30] M.M. Konai, J. Haldar, Fatty acid comprising lysine conjugates: anti-MRSA agents that display *in vivo* efficacy by disrupting biofilms with no resistance development, Bioconjugate Chem. 28 (2017) 1194–1204, https://doi.org/10.1021/acs.bioconjchem.7b00055.
[31] J. Hoque, R.G. Prakash, K. Paramanandham, B.R. Shome, J. Haldar, Biocompatible injectable hydrogel with potent wound healing and antibacterial properties, Mol. Pharm. 14 (2017) 1218–1230, https://doi.org/10.1021/acs.molpharmaceut.6b01104.
[32] B. Tarai, P. Das, D. Kumar, Recurrent challenges for clinicians: emergence of methicillin-resistant *Staphylococcus aureus,* vancomycin resistance, and current treatment options, J. Lab Phys. 5 (2013) 71–78, https://doi.org/10.4103/0974-2727.119843.
[33] D. Savoia, Plant-derived antimicrobial compounds: alternatives to antibiotics, Future Microbiol. 7 (2012) 979–990, https://doi.org/10.2217/fmb.12.68.
[34] A.C. Abreu, A.J. McBain, M. Simões, Plants as sources of new antimicrobials and resistance-modifying agents, Nat. Prod. Rep. 29 (2012) 1007–1021, https://doi.org/10.1039/c2np20035j.
[35] R. Gaur, V.K. Gupta, A. Pal, M.P. Darokar, R.S. Bhakuni, B. Kumar, *In vitro* and *in vivo* synergistic interaction of substituted chalcone derivatives with norfloxacin against methicillin resistant *Staphylococcus aureus*, RSC Adv. 5 (2014) 5830–5845, https://doi.org/10.1039/C4RA10842F.
[36] E. Gerits, E. Blommaert, A. Lippell, A.J. O'Neill, B. Weytjens, D. De Maeyer, A.C. Fierro, K. Marchal, A. Marchand, P. Chaltin, P. Spincemaille, K. De Brucker, K. Thevissen, B.P. Cammue, T. Swings, V. Liebens, M. Fauvart, N. Verstraeten, J. Michiels, Elucidation of the mode of action of a new antibacterial compound active against *Staphylococcus aureus* and *Pseudomonas aeruginosa*, PLoS One. 11; 11(5) (2016) e0155139, https://doi.org/10.1371/journal.pone.0155139.
[37] D.R. Nair, J. Chen, J.M. Monteiro, M. Josten, M.G. Pinho, H.G. Sahl, J. Wu, A. Cheung, A quinolinol-based small molecule with anti-MRSA activity that targets

bacterial membrane and promotes fermentative metabolism, J. Antibiot. (Tokyo) 70 (10) (2017) 1009–1019, https://doi.org/10.1038/ja.2017.79.
[38] S. Farooq, A.-T. Wahab, C.D.A. Fozing, A.-U. Rahman, M.I. Choudhary, Artonin I inhibits multidrug resistance in *Staphylococcus aureus* and potentiates the action of inactive antibiotics in vitro, J. Appl. Microbiol. 117 (2014) 996–1011, https://doi.org/10.1111/jam.12595.
[39] J.P. Dzoyem, H. Hamamoto, B. Ngameni, B.T. Ngadjui, K. Sekimizu, Antimicrobial action mechanism of flavonoids from *Dorstenia species*, Drug Discov. Ther. 7 (2013) 66–72.
[40] Y. Lv, J. Wang, H. Gao, Z. Wang, N. Dong, Q. Ma, A. Shan, Antimicrobial properties and membrane-active mechanism of a potential α-helical antimicrobial derived from cathelicidin PMAP-36, PLoS One 9 (2014) e86364, https://doi.org/10.1371/journal.pone.0086364.
[41] K. Okuda, T. Zendo, S. Sugimoto, T. Iwase, A. Tajima, S. Yamada, K. Sonomoto, Y. Mizunoe, Effects of bacteriocins on methicillin-resistant *Staphylococcus aureus* biofilm, Antimicrob. Agents Chemother. 57 (2013) 5572–5579, https://doi.org/10.1128/AAC.00888-13.
[42] Y. Hirakata, A. Kondo, K. Hoshino, H. Yano, K. Arai, A. Hirotani, H. Kunishima, N. Yamamoto, M. Hatta, M. Kitagawa, S. Kohno, M. Kaku, Efflux pump inhibitors reduce the invasiveness of *Pseudomonas aeruginosa*, Int. J. Antimicrob. Agents 34 (2009) 343–346, https://doi.org/10.1016/j.ijantimicag.2009.06.007.
[43] M.A. Farha, C.P. Verschoor, D. Bowdish, E.D. Brown, Collapsing the proton motive force to identify synergistic combinations against *Staphylococcus aureus*, Chem. Biol. 20 (2013) 1168–1178, https://doi.org/10.1016/j.chembiol.2013.07.006.